Moment-Reducing Hinge Details for the Bases of Bridge Columns

KUANG Y. LIM, DAVID I. MCLEAN, AND EDWARD H. HENLEY, JR.

Bridge foundations in seismic regions are designed to withstand the plastic hinge moments that develop at the bases of the bridge columns. In columns that are oversized for architectural or other reasons, this approach results in excessively large foundations. Various hinge details have been proposed to reduce the plastic moments transferred to the foundation and thereby reduce the size and cost of the foundation. The results of an experimental investigation of the seismic performance of bridge columns with moment-reducing details are presented. Tests were conducted on reinforced concrete column specimens subjected to axial load and cycled inelastic lateral displacements. The main parameters investigated in the testing program were different moment-reducing hinge details, the column aspect ratio, the level of axial load, and low-cycle fatigue characteristics. Columns with the moment-reducing details exhibited stable hinging behavior, even when subjected to repeated cycles at large displacement levels. The hinging behavior was similar to that for a conventional column with the same hinge dimensions and reinforcement. Flexure dominated the behavior of all the columns in this study, including those with an aspect ratio of 1.25. The level of axial load had only a limited effect on the behavior of the columns, with the moment-reducing details due to the confinement provided around the hinge region by the outer architectural column.

Bridge foundations in seismic regions are designed to withstand the plastic hinge moments that develop at the bases of the bridge columns. In columns that are oversized for architectural or other reasons, this approach results in excessively large foundations. Various hinge details for the bases of columns have been proposed, principally by bridge designers in the seismically active regions of the western United States, to reduce the plastic moments transferred to the foundations and thereby reduce the size and cost of the foundation.

The basic concept inherent in the modified hinge details is to provide a reduced moment capacity in the plastic hinging region at the bases of the columns. This is accomplished by placing a layer of easily compressed material at the base of the column, which provides partial discontinuity between the column and the footing. The discontinuity results in a smaller effective cross section at the column base and, thus, a reduced hinge capacity in the column. To a great extent, the modifications that have been suggested have been based on engineering judgment, and the behavior and safety of the moment-reducing details have not been fully established.

K. Y. Lim and D. I. McLean, Department of Civil and Environmental Engineering, Washington State University, Pullman, Wash. 99164–2910. E. H. Henley, Jr., Bridge and Structures Branch, Washington State Department of Transportation, Transportation Building KF-01, Olympia, Wash. 98504.

The results of an experimental investigation of the seismic performance of bridge columns with moment-reducing hinge details are presented. The hinge details investigated in this project are shown in Figure 1. Tests were conducted on reinforced concrete column specimens subjected to axial load and cycled inelastic lateral displacements. The main parameters investigated in the testing program were different moment-reducing hinge details, column aspect ratio, level of axial load, and low cycle fatigue characteristics.

EXPERIMENTAL PROGRAM

Reinforced concrete scale models of bridge columns were tested with different moment-reducing hinge details. The test specimens consisted of a single column member connected at the base to a rectangular footing. The specimens were subjected to increasing levels of cycled inelastic displacements under a constant axial load and were deflected in single curvature.

Experimental tests were performed on small-scale specimens of approximately 1/20 scale and moderate-scale specimens of approximately 1/6 scale. More than 50 small-scale specimens were tested. The small-scale tests provided a cost-efficient parametric study and also guided the selection of the parameters for the large-scale tests. Nine 1/6-scale specimens were tested. The larger, 1/6-scale tests resulted in a more realistic representation of the hinging behavior in actual bridge columns, and size effects were reduced when compared with the small-scale tests. Only the 1/6-scale test procedures and results are discussed in this paper. A detailed discussion of the test procedures and results for the small-scale study may be found elsewhere (*1*).

Test Specimens and Parameters

The test specimens were arranged in pairs: one specimen incorporated a hinge detail providing only horizontal discontinuity (CA detail) and the other specimen incorporated a hinge detail providing both vertical and horizontal discontinuity (WA detail). These details are shown in Figures 1a and 1b. The discontinuities between the column and the footing are provided by a layer of easily compressed material at the base of the column. Because only horizontal discontinuity is provided in the CA detail, the plastic hinging action in a column with this detail will be largely concentrated along a horizontal plane at the interface between the column and the footing. Both horizontal and vertical discontinuity are pro-

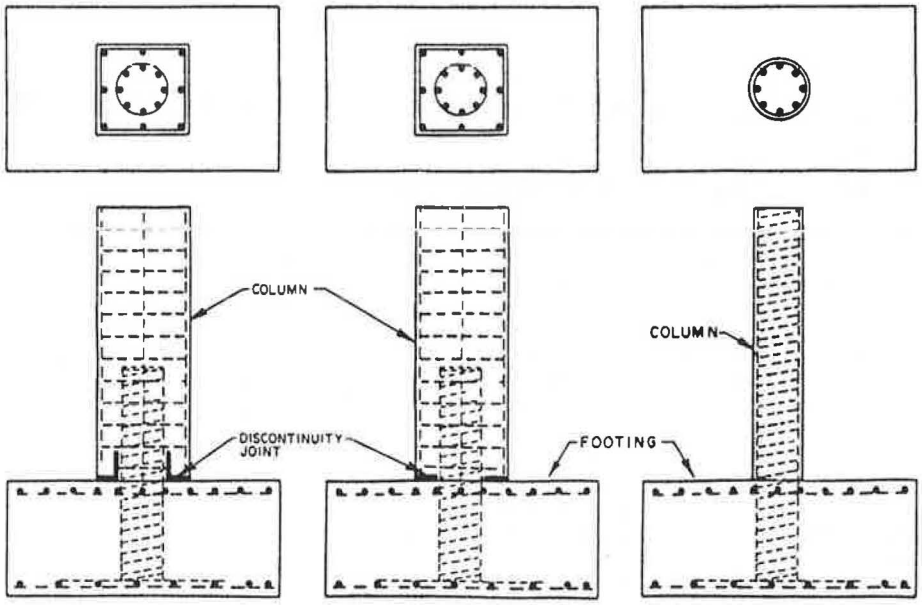

FIGURE 1 Hinge details investigated.

vided in the WA detail, with the objective of distributing the plastic stresses over a greater vertical length.

The testing program was carried out on four specimens incorporating the CA detail, four specimens incorporating the WA detail, and one reference or control column consisting of a column with the same dimensions and reinforcement as the hinge connection of the columns incorporating the moment-reducing hinge details (CON detail). Dimensions and reinforcement for a typical column specimen are shown in Figure 2.

Two column height-to-width ratios were investigated in the study: 1.25 and 2.5 measured with respect to the architectural column. The height of the architectural column, H, was varied while the cross-sectional dimensions of the column, D, were kept constant. Two levels of axial compression were studied: $P/(f'_c A_c) = 0.24$ and 0.35, where A_c is the cross-sectional area of the hinge connection measured out-to-out of the spiral. On the basis of actual designs of the moment-reducing hinge details and the results of the small-scale experimental study, a hinge longitudinal reinforcing ratio of 7.2 percent referenced to the area of the hinge connection and a hinge spiral reinforcing ratio of 1.5 percent were selected for use in all specimens.

The thickness of the horizontal discontinuity joint in the test specimens was 0.5 in. For the WA hinge detail, a vertical discontinuity joint with a height of 6 in. was also provided. On the basis of results from the small-scale tests, the horizontal joint thickness in both hinge details was increased to 1.0 in. at the outer edges of the column to allow the hinge to rotate without having the top of the footing contact the architectural column edge. The small-scale study indicated that hinge performance is independent of the shape of the architectural column if contact between the column edge and the footing is prevented. The discontinuity joints for columns with the CA and WA details are shown in Figure 3.

A summary of the details of the specimens of the testing program is given in Table 1.

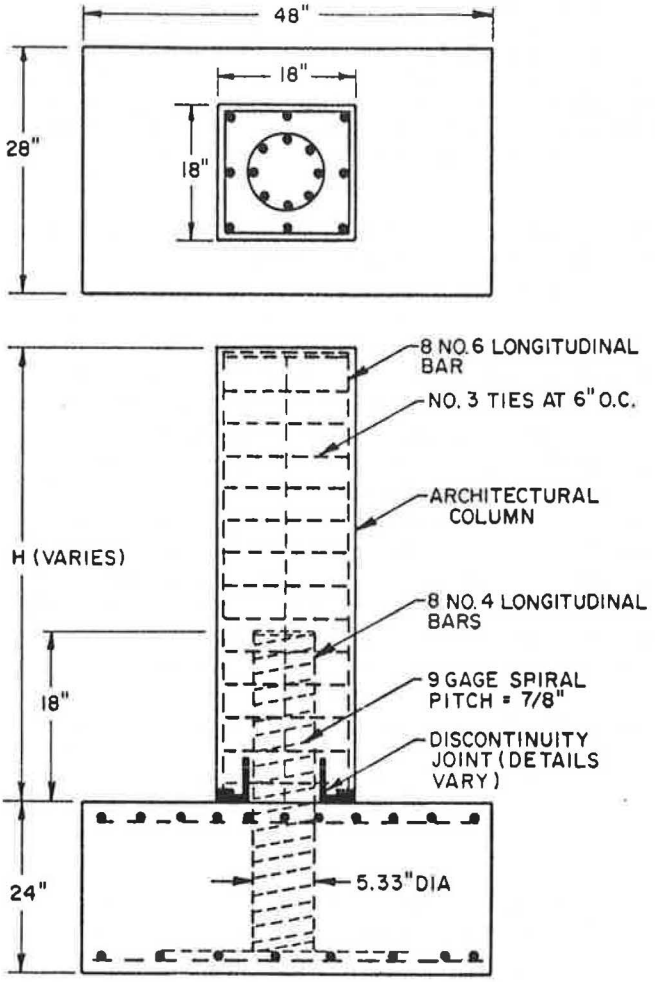

FIGURE 2 Typical dimensions and reinforcement of the column specimens.

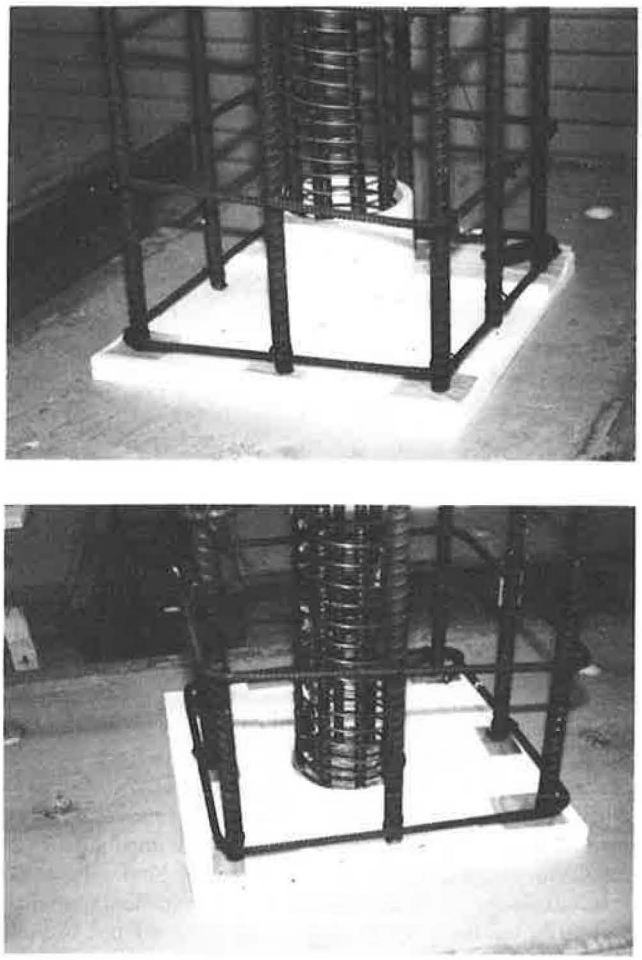

FIGURE 3 Hinge details before casting of the columns.

Materials

The concrete used in the specimens was a Washington State Department of Transportation Class AX mix (a typical mix used for bridge construction in Washington State). The concrete consisted of portland cement Type I/II, sand, river gravel coarse aggregate with a maximum size of ¾ in., water reducer, and an air-entraining agent. The mix resulted in an average compressive strength, measured at 28 days, of 5,000 psi.

Longitudinal reinforcement in the hinge region of the column specimens consisted of No. 4 ASTM Grade 60 reinforcing bars with a measured yield strength of approximately 65 ksi. Spiral reinforcement was provided in the hinge connection using 9 gauge (0.147-in.-diameter) ASTM A82 smooth bars with a measured yield strength of approximately 90 ksi.

The discontinuity joints were commercially manufactured preformed expanded polystyrene.

Test Apparatus, Instrumentation, and Procedures

After curing for approximately 28 days, the footing of a specimen to be tested was anchored to a laboratory strong floor. Axial force was first applied to the top of the column using a 55-kip actuator operated in force control. Axial forces were maintained at a constant level during a test. Lateral force was then applied slightly below the top of the column using a 22-kip actuator operated in displacement control. An analog signal of a prescribed ramp function was generated using a personal computer and sent to the servocontroller of the actuator. Figures 4 and 5 show the test setup.

Actuator loads and displacements were monitored during the tests. Linear variable displacement transformers (LVDTs) were mounted to the sides of the columns to measure the rotation of the column base. Strain gauges were used to monitor the strains in the longitudinal and spiral reinforcement within the hinging region. All data were recorded intermittently on the same personal computer used to generate control signals for the horizontal actuator.

The determination of the yield displacement, Δy, and the loading sequence was similar to the procedures used by Priestley and Park, Ang et al., and Park and Blakely (*2–4*). However, on the basis of preliminary tests, it was found that the ultimate moment capacities and stiffnesses, and hence the yield displacements, varied in columns with different details. In order to better compare the hinging behavior of columns with the CA and WA details, it was decided that parallel sets of columns would be subjected to the same displacement history. Thus, the same displacement value was defined as the yield displacement for columns incorporating different hinge

TABLE 1 SUMMARY OF THE TESTING PROGRAM

Specimen No.	Variable Studied	Aspect Ratio (H/D)	Axial Load (P/f'_cA_c)	Yield Displacement (in.)	Measured Yield Moment (in.-kips)	Measured Peak Moment (in.-kips)	Maximum Applied Shear Load (kips)
CA1	aspect ratio	2.50	0.24	0.30	181	270	6.0
WA1	"	2.50	0.24	0.30	133	212	4.7
CON2	hinge detail	*	0.24	0.15	93	209	9.3
CA2	"	1.25	0.24	0.15	162	279	12.4
WA2	"	1.25	0.24	0.15	142	250	11.1
CA3	axial load	1.25	0.35	0.15	166	277	12.3
WA3	"	1.25	0.35	0.15	135	240	10.7
CA4	low-cycle fatigue	1.25	0.24	0.15	138	271	12.0
WA4	"	1.25	0.24	0.15	130	236	10.5

* circular control column with the same height as Units CA2 and WA2

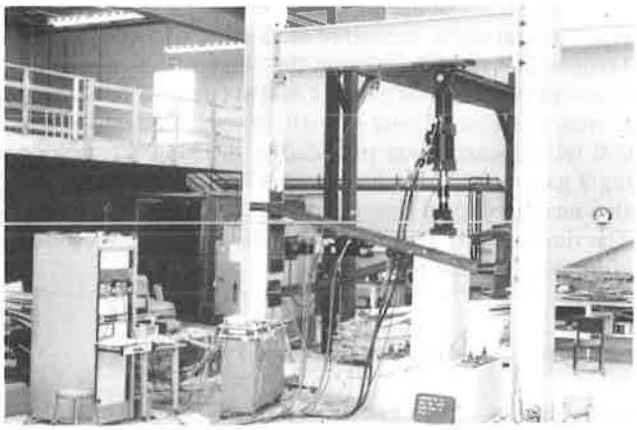

FIGURE 4 Test setup.

details but with the same aspect ratio. The typical loading sequence used for the tests was two cycles at displacement ductility factors (i.e., multiple values of Δy) of μ = 1, 2, 4, 6, 8, 10, and 12. Figure 6 shows the typical loading sequence.

RESULTS AND DISCUSSION

A summary of the test results for all specimens is presented in Table 1. Column performance was evaluated with respect to the moment capacity and displacement ductility attained, the overall hysteresis behavior, and degradation and energy dissipation characteristics. Rather than a discussion of the results for each specimen individually, results for groups of specimens are presented to facilitate correlation of the influence of various parameters with column performance and to obtain behavioral trends.

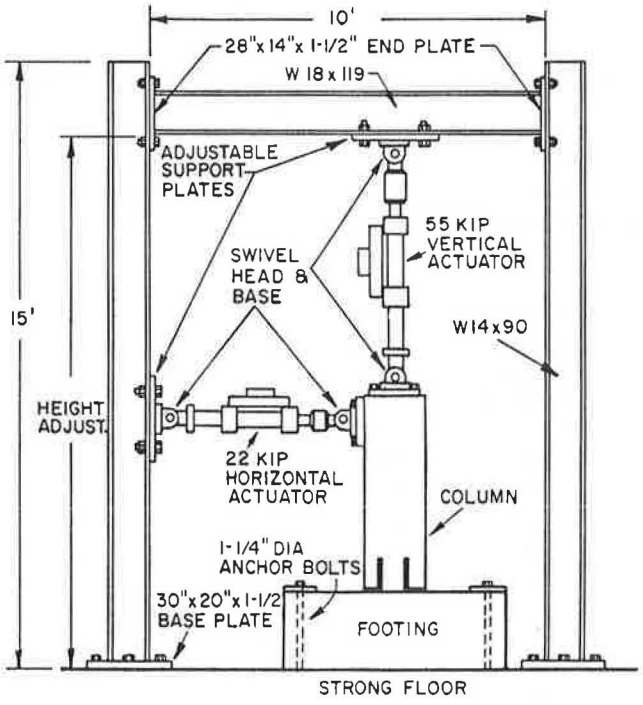

FIGURE 5 Schematic drawing of the test setup and reaction frame.

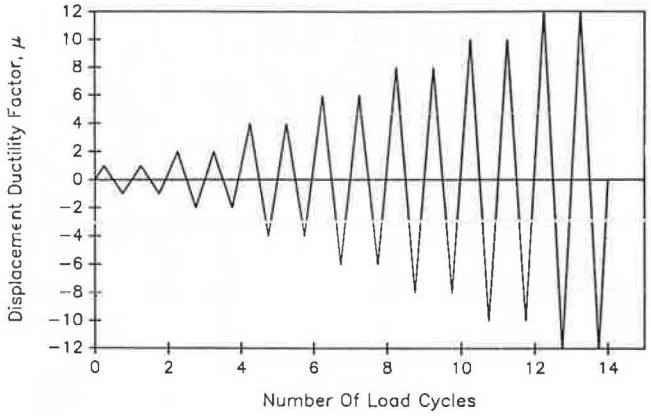

FIGURE 6 Typical loading sequence.

General Behavior

Tests were performed on columns incorporating a WA detail (Unit WA2), a CA detail (Unit CA2), and a circular control column (Unit CON2) with the same dimensions and reinforcement as the inner hinge of the modified columns. These columns were subjected to an axial load level of $0.24f'_cA_c$, and the columns had an aspect ratio of 1.25. The load-displacement hysteresis curves for Units WA2, CA2, and CON2 are shown in Figures 7, 8, and 9, respectively. The lateral loads presented are the true lateral loads on the specimens, including P-Δ effects and secondary effects from the axial load. The hysteresis curves for all three specimens show excellent stability even at displacement levels of μ = 12. No evidence of any sudden drop in load-carrying capability was observed, and the plastic hinges continued to absorb energy throughout the tests.

Figure 10 shows the plots of the shear strength envelope curves for these columns, which is obtained by plotting the maximum shear force attained at each peak displacement level with respect to that displacement. For Units WA2 and CA2, very little degradation in strength is observed. However, some degradation can be seen in Unit CON2 begining after μ = 4. Also from Figure 10, it can be seen that Unit CA2 exhibited the greatest stiffness and Unit CON2, the least stiffness. Two reasons can be cited for the difference in stiffness observed in these specimens. First, the elastic stiffness of the control column is less than that of the architectural columns with the moment-reducing details. Second, the moment-reducing details may have the effect of "pinching" the rebar crossing the interface between the column and the footing, particularly with the CA detail, thereby introducing larger strain values in the longitudinal reinforcement of the moment-reducing details. Readings from strain gauges mounted on the longitudinal bars at the bases of the columns indicated that the strains were consistently higher in Units CA2 and WA2 than in Unit CON2 for the same level of displacement. The largest strain values, for the same level of displacement, were recorded in UnitCA2.

Effects of Column Aspect Ratio

To evaluate the effects of column aspect ratio on the behavior of the modified hinges, test results for columns with aspect

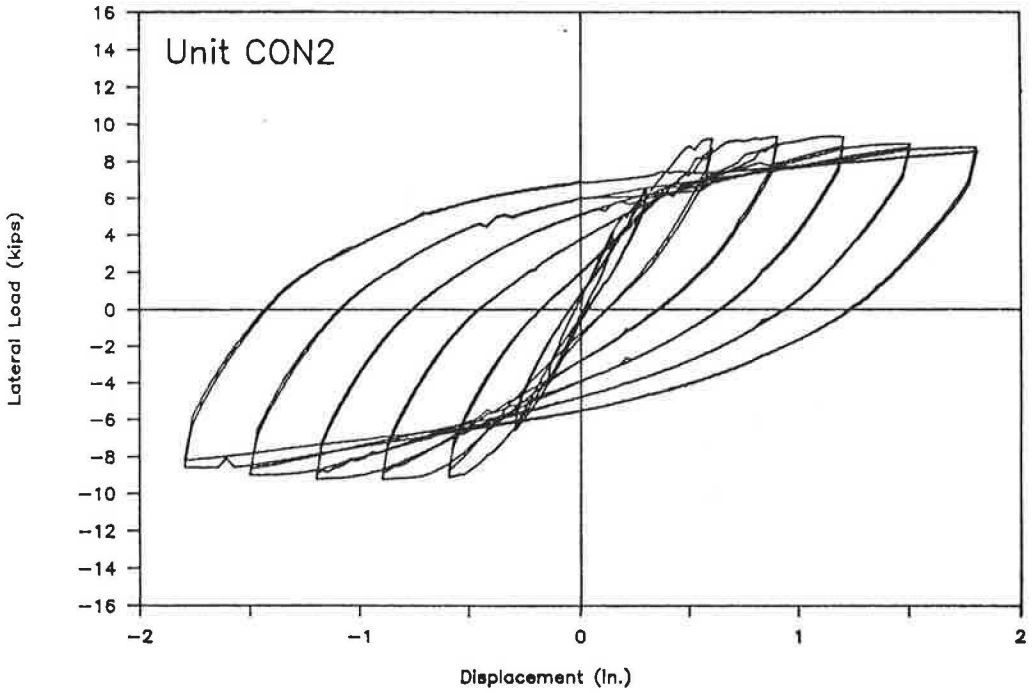

FIGURE 9 Lateral load-displacement hysteresis curves for Unit CON2.

in strength occurred in the columns with the higher aspect ratio, particularly for the column with the WA detail. It can also be seen that the drop in strength from the first to the second cycle of loading for the columns incorporating the CA detail was approximately constant for the two aspect ratios. However, the drop was greater in the shorter column incorporating the WA detail.

Effects of Axial Load Level

To examine the effect of the axial load levels on the modified column performance, Units WA2 and CA2 and Units WA3 and CA3 were tested with axial load levels of $0.24f'_cA_c$ and $0.35f'_cA_c$, respectively. The hysteresis curves for Units WA3 and CA3 are shown in Figures 15 and 16, respectively. Comparing these hysteresis curves with those for Units WA2 and CA2, it can be seen that there is only a small difference between the curves for the specimens with the WA details, and there is virtually no difference in the curves for the specimens with the CA details.

Figures 17 and 18 show the shear strength envelope curves for Units WA2 and WA3 and Units CA2 and CA3, respectively. In the columns with the WA detail, the larger axial load resulted in a greater drop in strength. In the columns with the CA detail, axial load seemed to have little effect on the strength. The reason that these columns are relatively unaffected by axial load level may be the considerable confining effect provided around the hinge region by the outer architectural column, particularly with the CA detail.

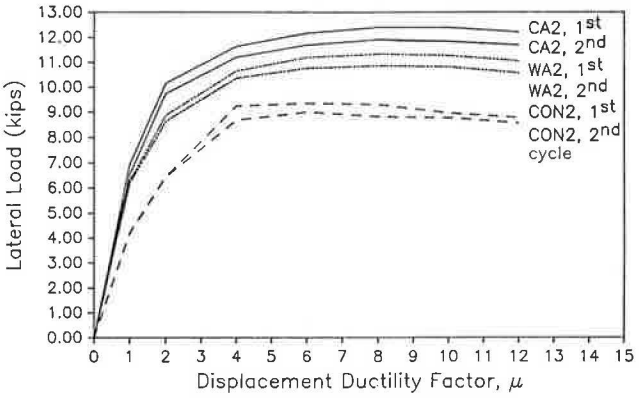

FIGURE 10 Shear strength envelope curves for Units CON2, WA2, and CA2.

Effects of Low-Cycle Fatigue

Tests were performed on Column Units WA4 and CA4 to evaluate the low-cycle fatigue characteristics of the moment-reducing hinge details. Both units were cycled to a displacement level of $\mu = 10$ and then subjected to multiple cycles at this displacement level. The hysteresis curves for Units WA4 and CA4 are shown in Figures 19 and 20, respectively. For both specimens, very little degradation occurred after the completion of the second cycle at $\mu = 10$. The hinges continued to exhibit stable plastic behavior even after being cycled up to 16 times at this displacement level.

Repeatability of Results

Units WA4 and CA4 were constructed identically to Units CA2 and WA2. The two sets of columns were also loaded identically through two cycles of loading to a displacement ductility level of $\mu = 10$. Hence, comparing the results from

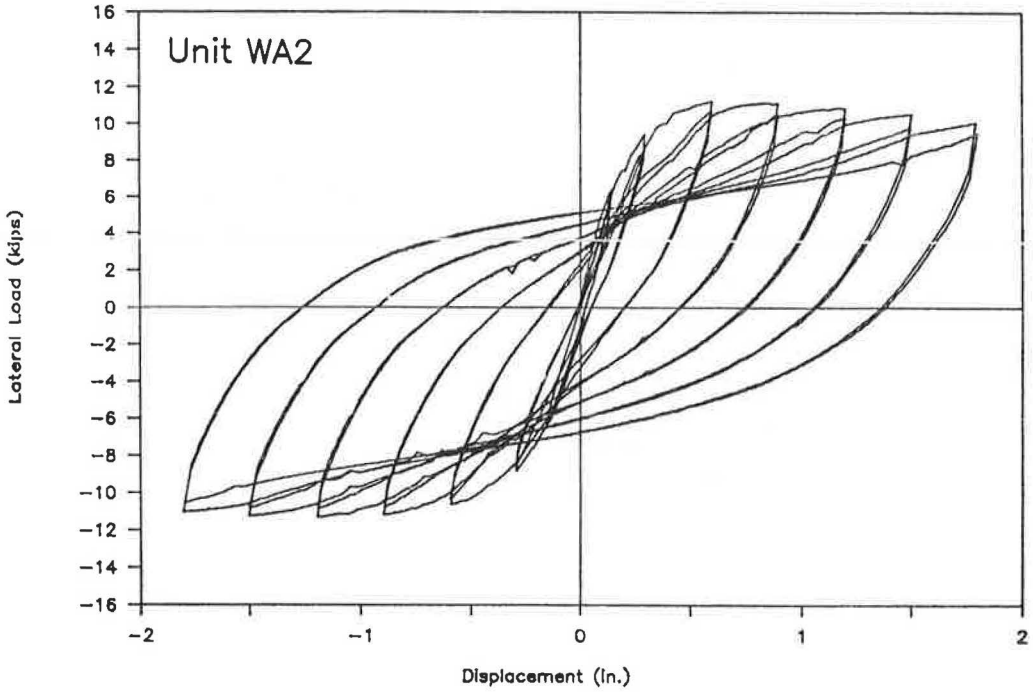

FIGURE 7 Lateral load-displacement hysteresis curves for Unit WA2.

ratios of 2.5 (Units WA1 and CA1) and 1.25 (Units WA2 and CA2) were compared. The hysteresis curves for Units WA1 and CA1 are shown in Figures 11 and 12, respectively. The hysteresis curves for the specimens with the higher aspect ratio are similar to those for the shorter specimens, indicating that flexure dominated the behavior of both sets of specimens. However, it can be seen in the plots that the curves for Unit CA1 are somewhat narrower than those for Unit WA1, indicating decreased energy dissipation characteristics in the column with the CA detail.

The shear strength envelope curves for Units WA1 and WA2 and Units CA1 and CA2 are shown in Figures 13 and 14, respectively. To account for the different lateral load levels associated with columns of different heights, the shear force, V, is plotted normalized with respect to the yield shear force, V_y. It can be seen in Figures 13 and 14 that greater degradation

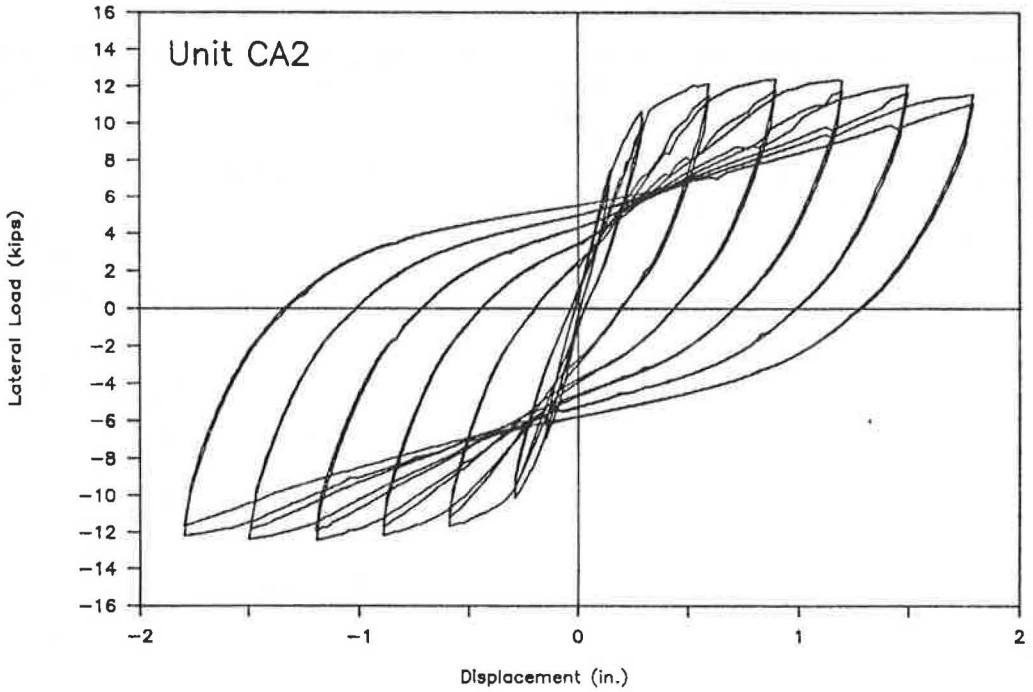

FIGURE 8 Lateral load-displacement hysteresis curves for Unit CA2.

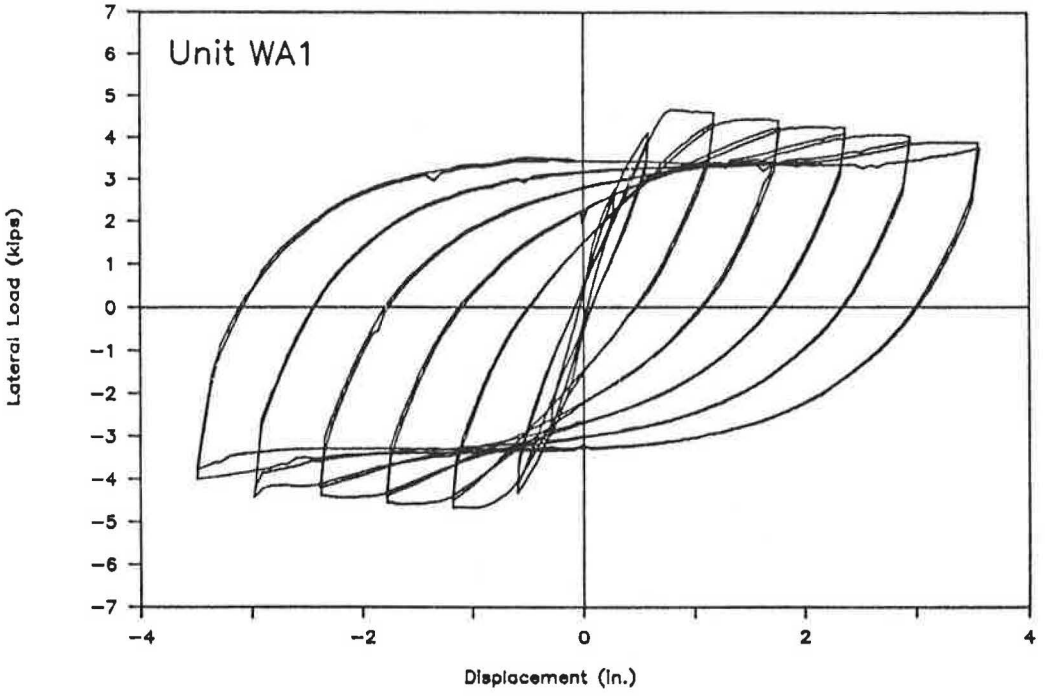

FIGURE 11 Lateral load-displacement hysteresis curves for Unit WA1.

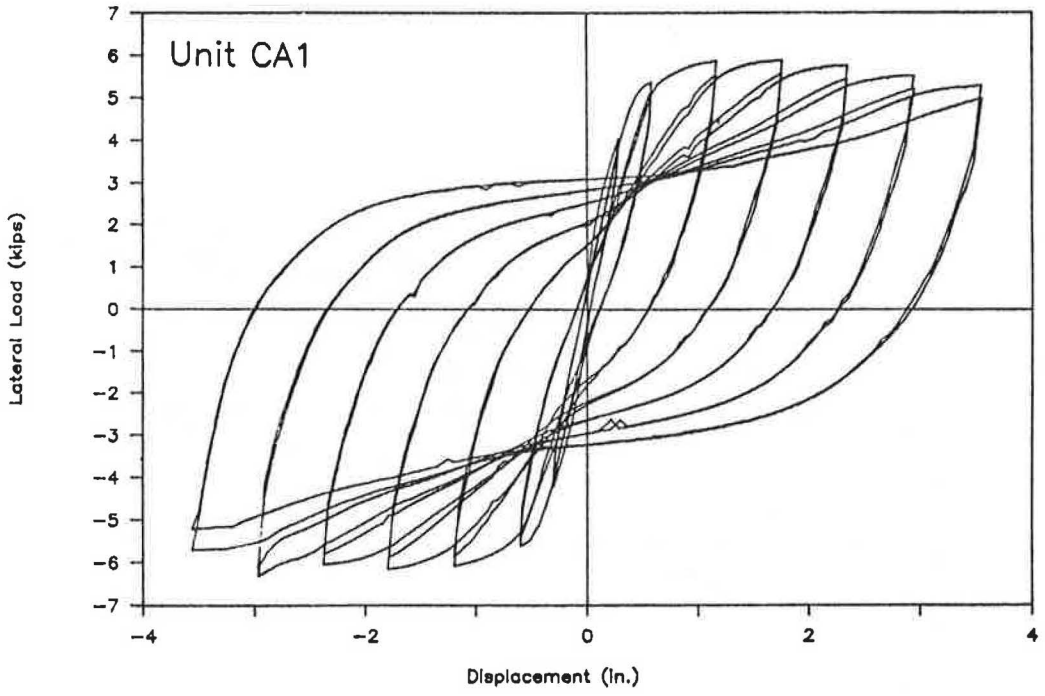

FIGURE 12 Lateral load-displacement hysteresis curves for Unit CA1.

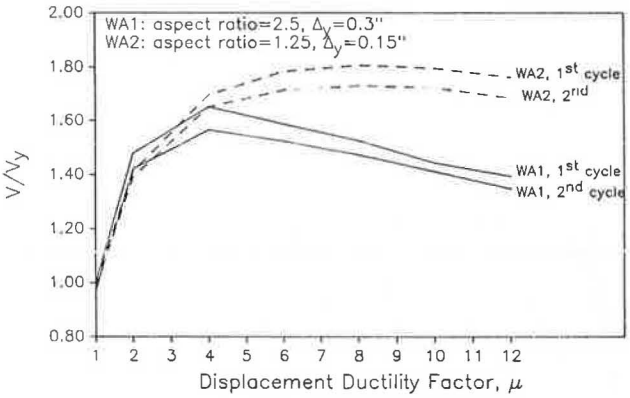

FIGURE 13 Shear strength envelope curves for Units WA1 and WA2.

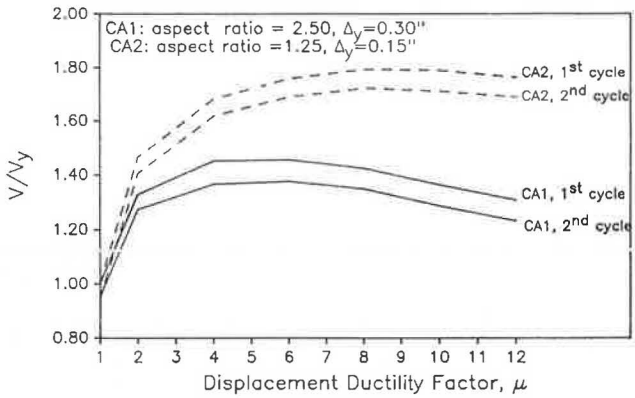

FIGURE 14 Shear strength envelope curves for Units CA1 and CA2.

these columns provides a measure of the repeatability of the test results. The shear strength envelope curves for Units WA2 and WA4 and Units CA2 and CA4 are shown in Figures 21 and 22, respectively. It can be seen that there is close agreement between the results from the two sets of tests.

Comparison of Energy Dissipation Characteristics

The energy dissipated by a column during a particular load cycle is represented by the area enclosed by the load-displacement hysteresis curve. The energy dissipated by a perfectly elastoplastic system during a complete displacement cycle, as shown in Figure 23, is the area of the parallelogram *BCDE*. For a particular displacement ductility factor, μ, the ideal plastic energy dissipated, E_p, can be computed as

$$E_p = 4(\mu - 1)V_p\Delta_y$$

where V_p is the maximum shear force attained at that displacement level (*3*).

In order to evaluate quantitatively the energy dissipation capability of the various hinge details, the measured energy dissipation was divided by the E_p-value of the column for the same displacement ductility factor. This ratio will be referred to as the relative energy dissipation index. Plots of E/E_p values versus the displacement ductility factor, μ, for Units WA2, CA2, and CON2 are shown in Figure 24. The low values of E/E_p at $\mu = 2$ and $\mu = 4$ for the control column, Unit CON2, are due to the inexactness in defining the actual yield dis-

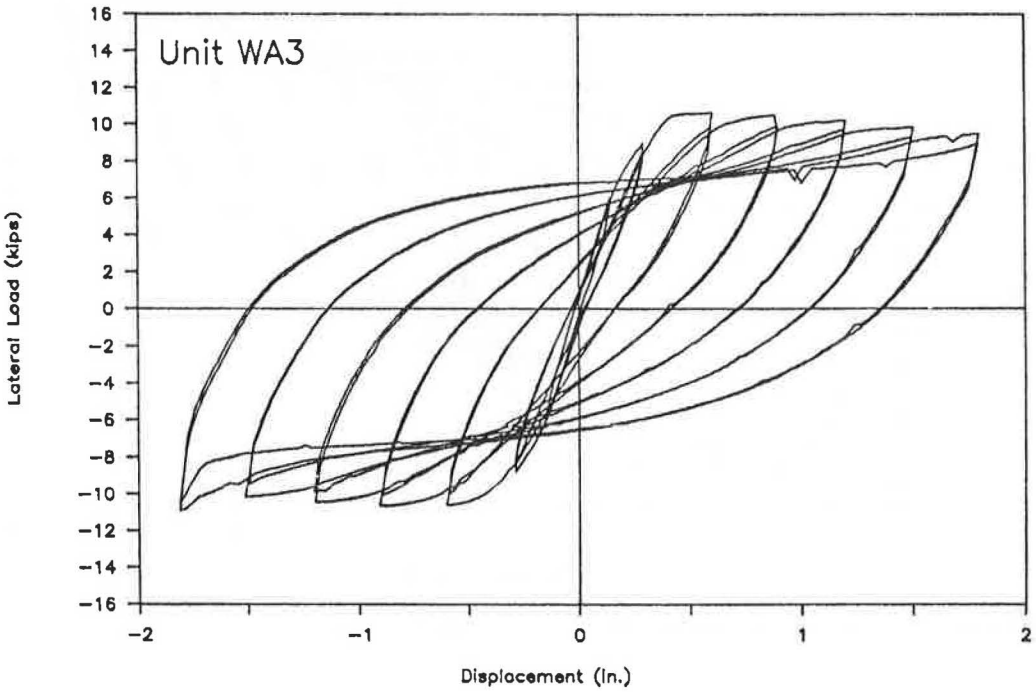

FIGURE 15 Lateral load-displacement hysteresis curves for Unit WA3.

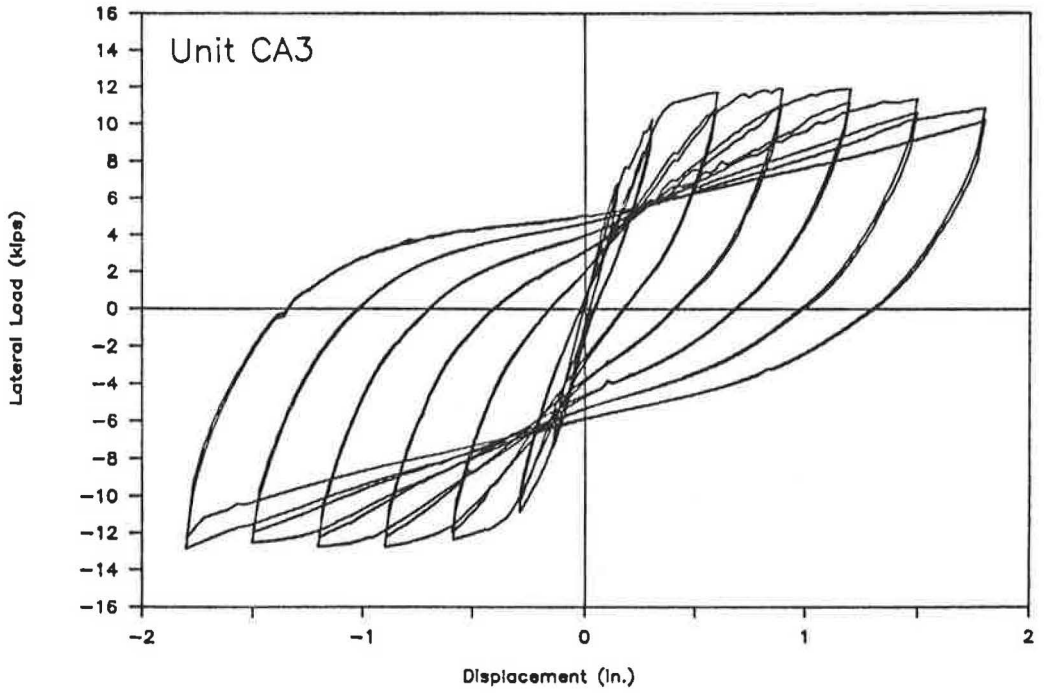

FIGURE 16 Lateral load-displacement hysteresis curves for Unit CA3.

placement in the different columns, with the result that the response of Unit CON2 is still largely elastic at these displacement levels. It can be seen in Figure 24 that the energy dissipation effectiveness is greatest for Unit CON2 and least for Unit CA2. The reduced effectiveness in the columns with the moment-reducing details may be due to a confining of the plastic action (i.e., reduction in length over which the plastic hinge is developing) at the base of the column, particularly for the CA detail.

SUMMARY AND CONCLUSIONS

The following observations and conclusions were made about the major variables investigated in this study.

1. When subjected to cycled inelastic displacements under constant axial load, the columns of this study with moment-reducing plastic hinge details, both those with the WA detail and those with the CA detail, displayed a hinging behavior that was very similar to the hinging behavior of an unmodified column with the same dimensions and reinforcement. Even at displacement levels of $\mu = 12$, the columns exhibited stable load-deflection hysteresis curves and continued to absorb energy.

2. Columns with the CA moment-reducing detail developed larger strain values in the longitudinal bars for the same level of displacement than did the columns with either the WA moment-reducing detail or the unmodified (control) detail. In addition, columns with the CA detail had lower energy dissipation effectiveness compared with the effectiveness of

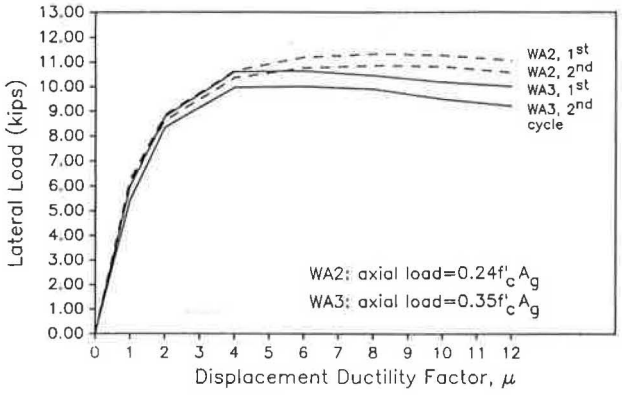

FIGURE 17 Shear strength envelope curves for Units WA2 and WA3.

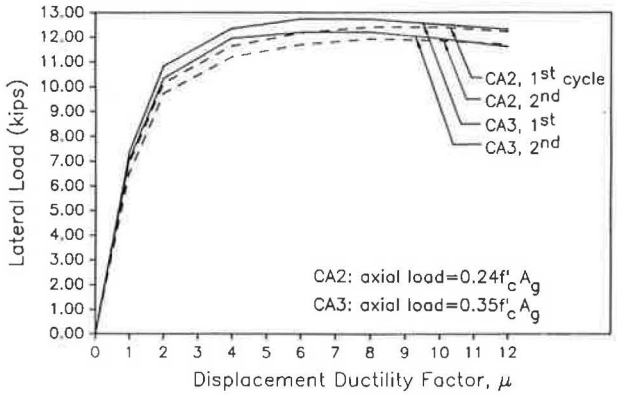

FIGURE 18 Shear strength envelope curves for Units CA2 and CA3.

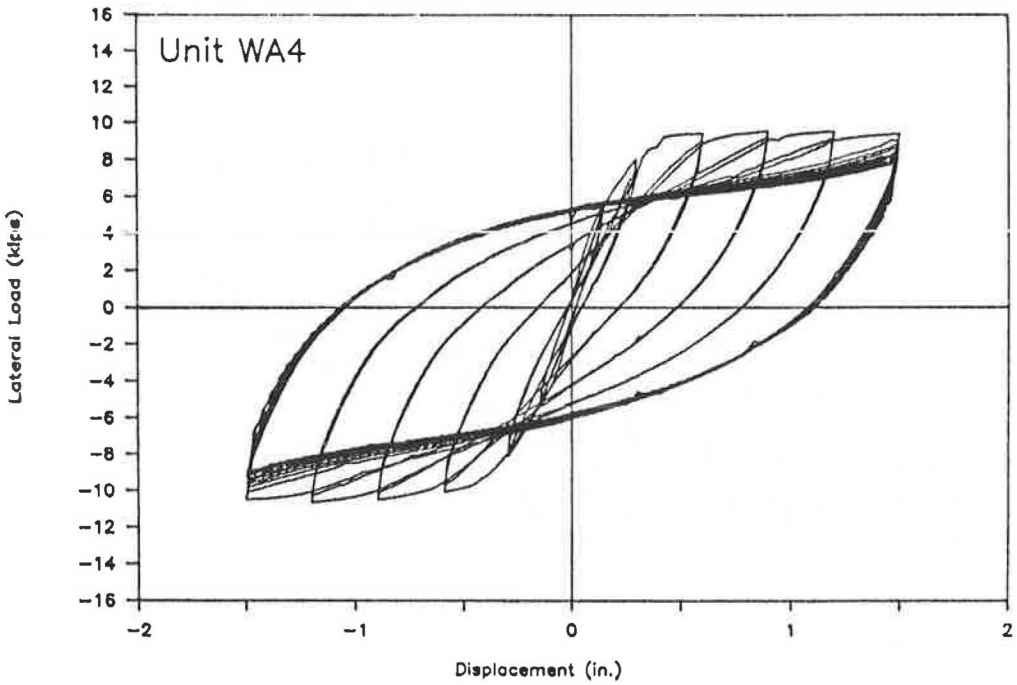

FIGURE 19 Lateral load-displacement hysteresis curves for Unit WA4.

the columns with the other details. Both the larger strain values and the lower energy dissipation effectiveness may be a result of a confining of the plastic hinging action in the columns with the CA detail.

3. Flexure dominated the behavior of all the columns of this study, including those with an aspect ratio of 1.25. However, the lower aspect ratio resulted in a greater drop in strength between the first and second cycle of loading at a particular displacement level in the columns with the WA detail.

4. Increasing the magnitude of the axial load by approximately 50 percent resulted in a slightly greater degradation of shear strength in the columns with the WA detail. However, the columns with the CA details were unaffected by the

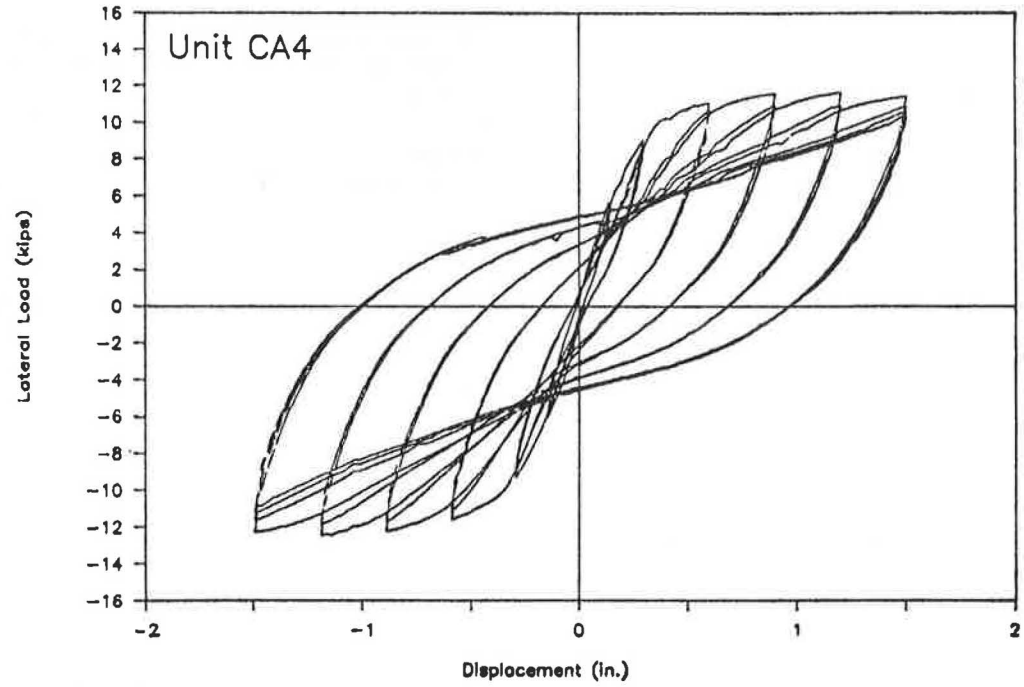

FIGURE 20 Lateral load-displacement hysteresis curves for Unit CA4.

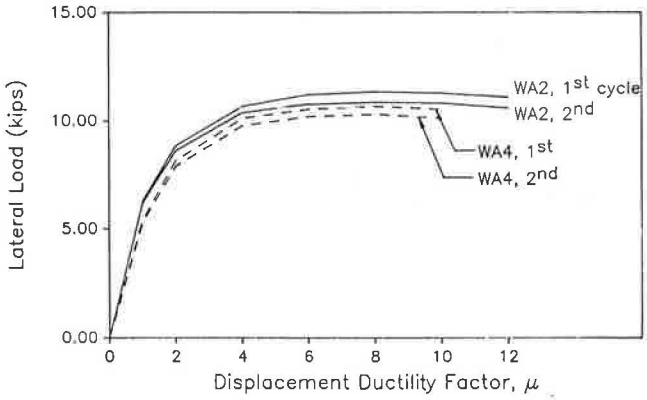

FIGURE 21 Shear strength envelope curves for Units WA2 and WA4.

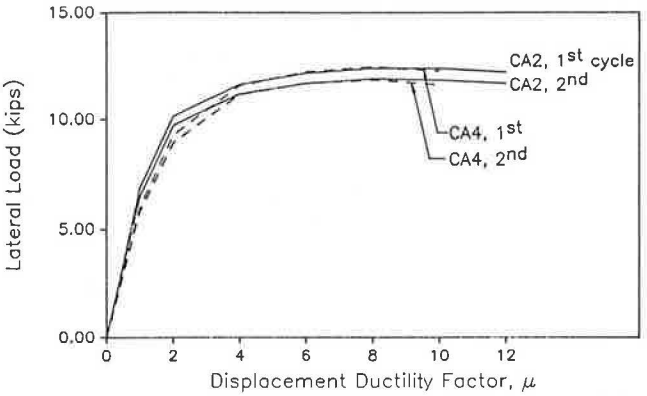

FIGURE 22 Shear strength envelope curves for Units CA2 and CA4.

increased axial load. This lack of effect was attributed to the confinement provided around the hinge by the outer architectural column.

5. In the low-cycle fatigue tests, no evidence of distress was observed in the columns with either the WA or CA details when units were cycled up to 16 times at a displacement level of $\mu = 10$.

ACKNOWLEDGMENTS

The research presented in this paper was funded by the Washington State Transportation Center (TRAC). The authors acknowledge the valuable advice and assistance of several people, including Umesh Vasishth of Arvid Grant and Associates Consulting Engineers; Robert Chen of the Washington State Department of Transportation; and Kurt Nelson, Yung-Ho Won, John Peterson, and Greg Lisle, graduate and undergraduate students in the Department of Civil and Environmental Engineering at Washington State University.

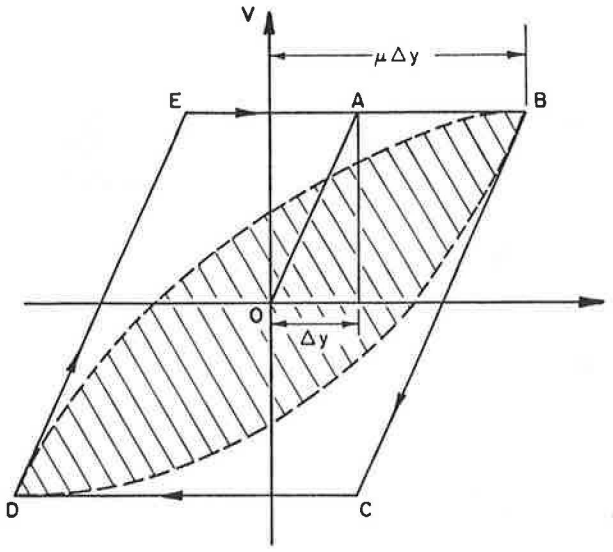

FIGURE 23 Actual and idealized perfectly elastoplastic hysteresis curves.

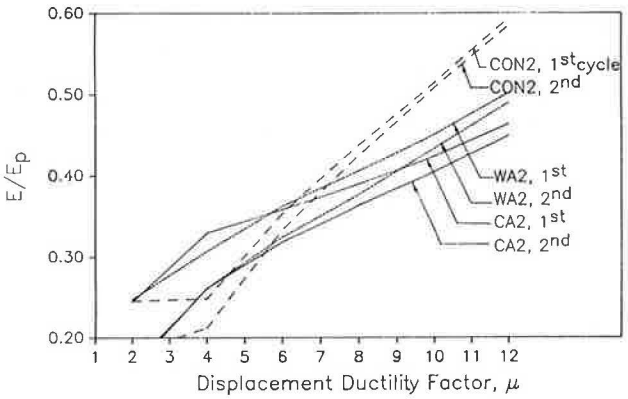

FIGURE 24 Relative energy dissipation index curves for Units CON2, WA2, and CA2.

REFERENCES

1. K. Y. Lim, D. I. McLean, and E. H. Henley. *Plastic Hinge Details for the Bases of Bridge Columns: Small-Scale Model Study*. Interim Project Report. Washington State Department of Transportation, Olympia, April 1989.
2. M. J. N. Priestley and R. Park. Strength and Ductility of Concrete Bridge Columns Under Seismic Loading. *ACI Structural Journal*, Jan.–Feb. 1987.
3. B. G. Ang, M. J. N. Priestley, and T. Pauley. *Seismic Shear Strength of Circular Bridge Piers*. Research Report 85-5. Department of Civil Engineering, University of Canterbury, Christchurch, New Zealand, July 1985.
4. R. Park and R. W. G. Blakely. *Seismic Design of Bridges: Bridge Seminar 1979*, Summary Vol. 3. Structures Committee, Road Research Unit, National Roads Board, New Zealand, 1979.

Publication of this paper sponsored by Committee on Concrete Bridges.